

Search for $K_S^0 \rightarrow \mu^+ \mu^-$ and rare kaon decay prospects with LHCb

Miguel Ramos Pernas

miguel.ramos.pernas@cern.ch

November 19, 2020



- Introduction
 - Current picture of strange decays
 - The LHCb detector to study strange decays
- Search for the $K_S^0 \rightarrow \mu^+ \mu^-$ decay using 2011–2012 (Run 1) and 2016–2018 (Run 2) data collected by the LHCb detector:
 - Topology, backgrounds, ...
 - Normalization and systematic uncertainties
 - The dimuon invariant mass fit
- Other analyses involving strange decays.
- Future of strange decays at LHCb:
 - Keys to study strange decays in the upgraded LHCb.
 - Prospects for the near and far future



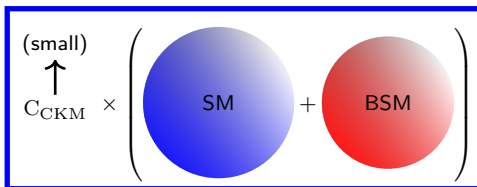
Strange decays

Strange decays

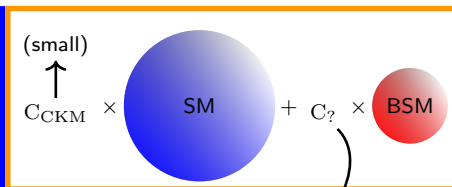
Decays of hadrons containing the s quark play a major role in particle physics:

- They were of high relevance in the past, with analysis that lead to the prediction of the c quark, CP-violation and the third family of quarks.
- If the BSM scale is at $\mathcal{O}(\text{TeV})$, it might only be seen if there are new sources of flavor violation.
- $s \rightarrow d$ transitions have the strongest suppression in the SM, of $V_{td}V_{ts}^* \sim 10^{-4}$.
- In a Non-Minimal-Flavor-Violating (Non-MFV) paradigm they are highly sensitive to BSM contributions.

MFV paradigm



Non-MFV paradigm



If $C_? \sim 1$ bounds from strange decays go up to 10^5 TeV

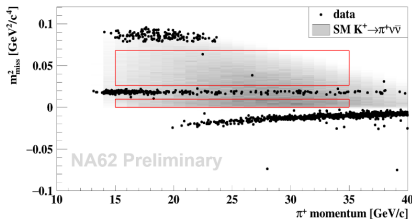
The current picture of strange decays

Golden channels $K^\pm \rightarrow \pi^\pm \nu \bar{\nu}$ and $K_L^0 \rightarrow \pi^0 \nu \bar{\nu}$:

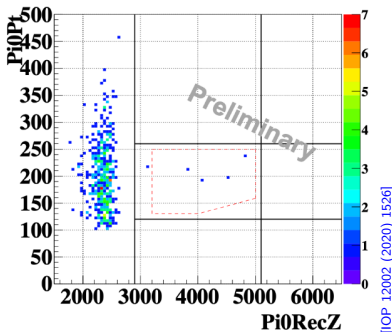
- Highly suppressed in the SM $\mathcal{B} \sim 10^{-11}$, and challenging from the experimental point of view.
- Very clean from the theoretical point of view, errors $\sim 2\%$.
- Currently at the SM sensitivity.

Complementary measurements in other frontiers:

- **Very rare decays, like $K_S^0 \rightarrow \mu^+ \mu^-$.**
- Possible anomaly in CP-violating quantities (ε'/ε).
- LFU and LFV ($K^+ \rightarrow \pi^+ \mu^+ \mu^-$, $K^+ \rightarrow \pi^+ e^+ e^-$, $K^+ \rightarrow \pi^+ e^- \mu^+$).



[IOP 12003 (2020) 1526]

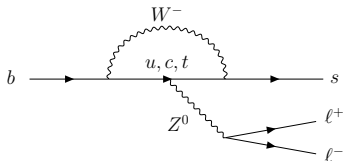
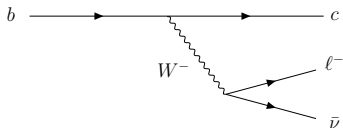
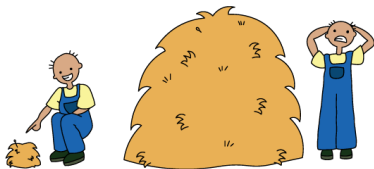


[IOP 12002 (2020) 1526]

Very rare decays to search for new physics

Indirect searches allow us to reach higher energy scales and access new particles without producing them in the laboratory.

Higher sensitivity in searches for BSM with low background (e.g. SM signal) levels:



- Tree level:

- Higher SM signal, $\mathcal{B} \sim 10\%$ (bigger haystack).
- Studies systematically limited (or close to be).
- Challenging to accommodate New Physics with the current constraints.

- Loop level:

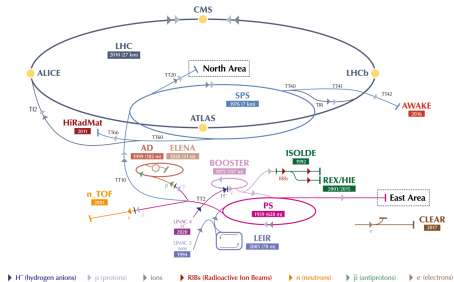
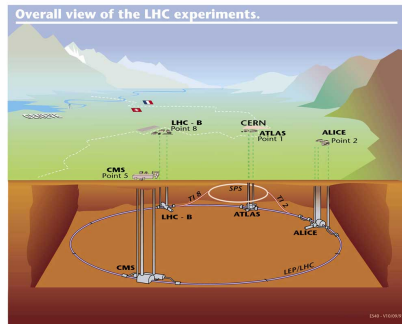
- Smaller SM signal, $\mathcal{B} \sim 10^{-8}$ (smaller haystack).
- Statistically limited.
- More rich from the theoretical point of view.

The LHCb detector



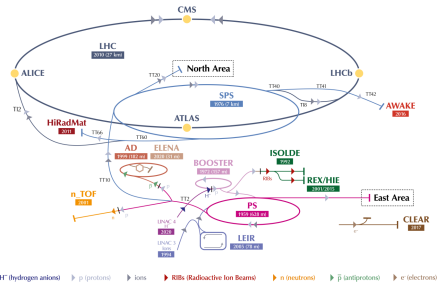
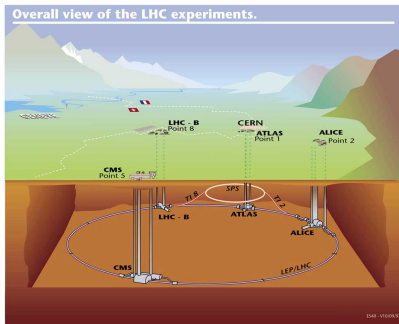
LHCb: a forward-arm spectrometer at the LHC

- Located at the Large Hadron Collider (LHC).
- Initially designed for the study of b and c hadron decays arising from proton-proton collisions.
- Complementary to other b -physics experiments: Belle, Babar, ...



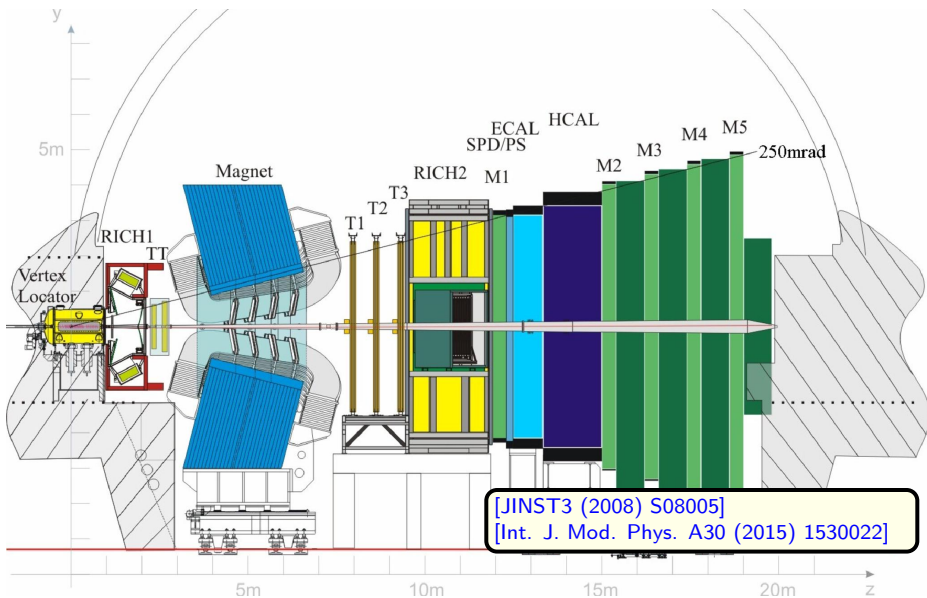
LHCb: a forward-arm spectrometer at the LHC

- Located at the Large Hadron Collider (LHC).
- Initially designed for the study of b and c hadron decays arising from proton-proton collisions.
- Complementary to other b -physics experiments: Belle, Babar, ...

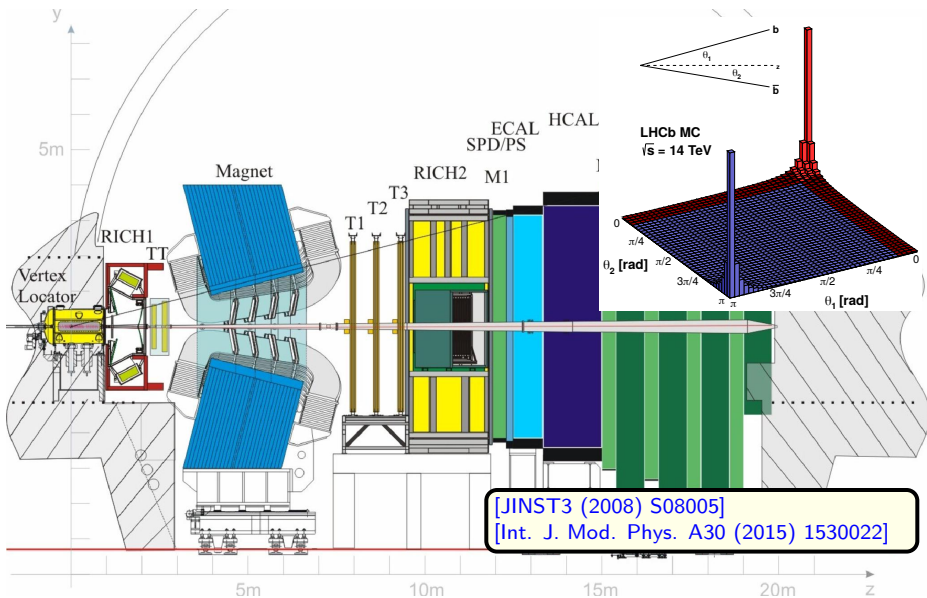


- LHCb can be considered as a general-purpose detector in the forward region.
- Profit from the flexibility and the capability to easily change its configuration.
- Increased physics program: exotic signatures, proton-ion, **strange decays**, ...

The LHCb detector



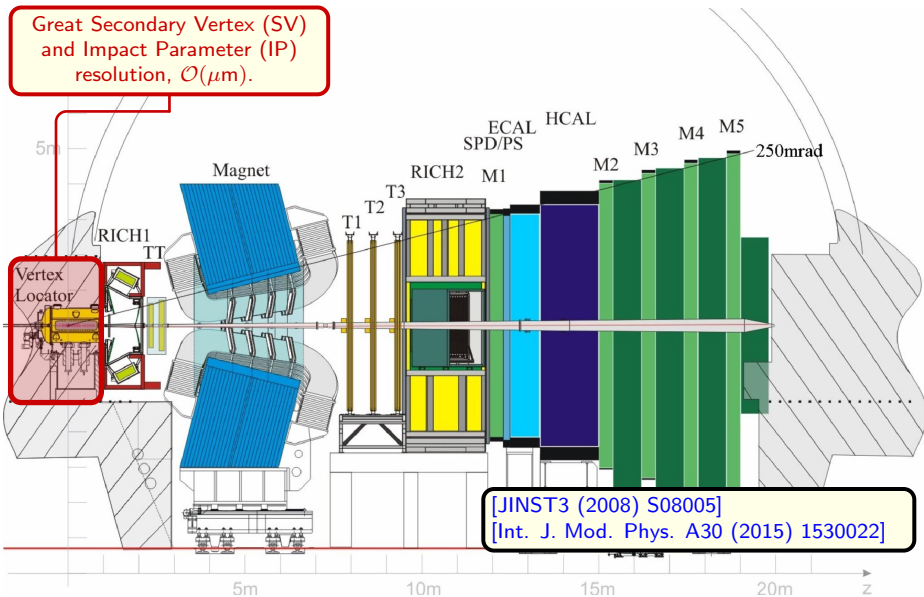
The LHCb detector



[JINST3 (2008) S08005]
 [Int. J. Mod. Phys. A30 (2015) 1530022]

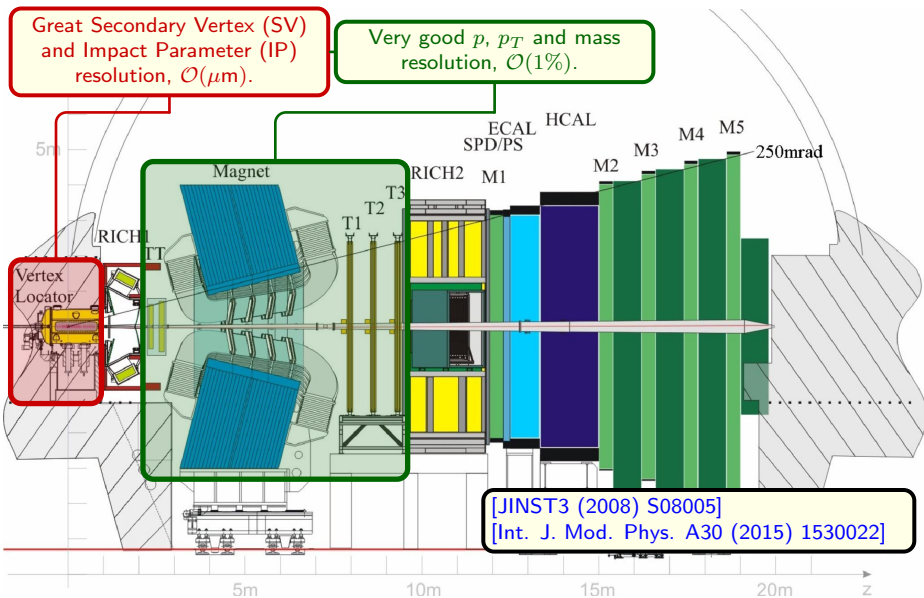
The LHCb detector

Great Secondary Vertex (SV)
and Impact Parameter (IP)
resolution, $\mathcal{O}(\mu\text{m})$.

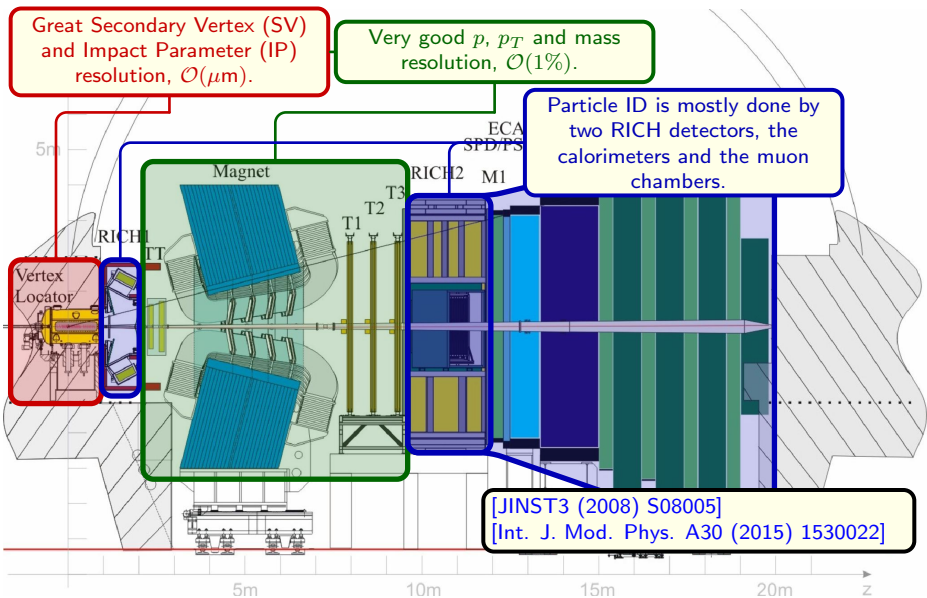


[JINST3 (2008) S08005]
[Int. J. Mod. Phys. A30 (2015) 1530022]

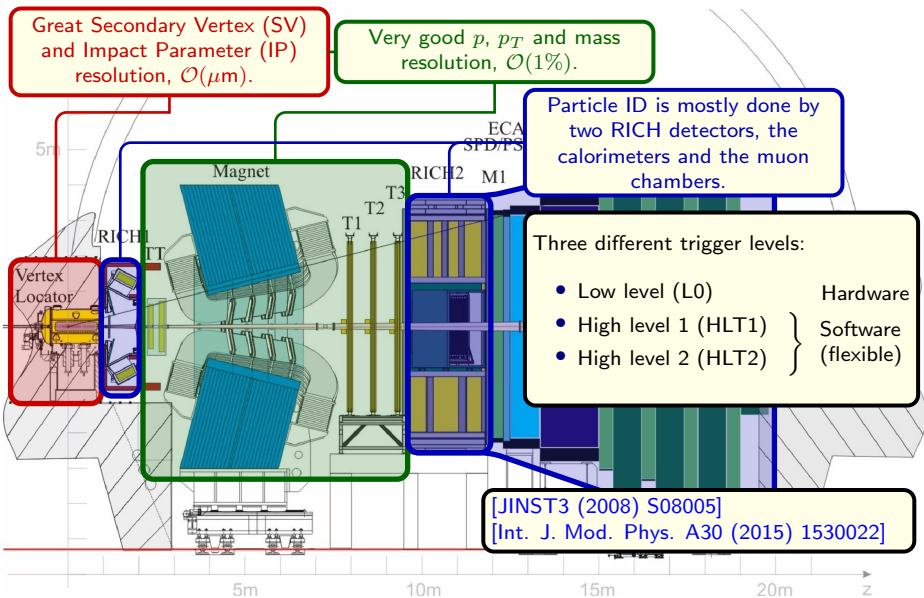
The LHCb detector



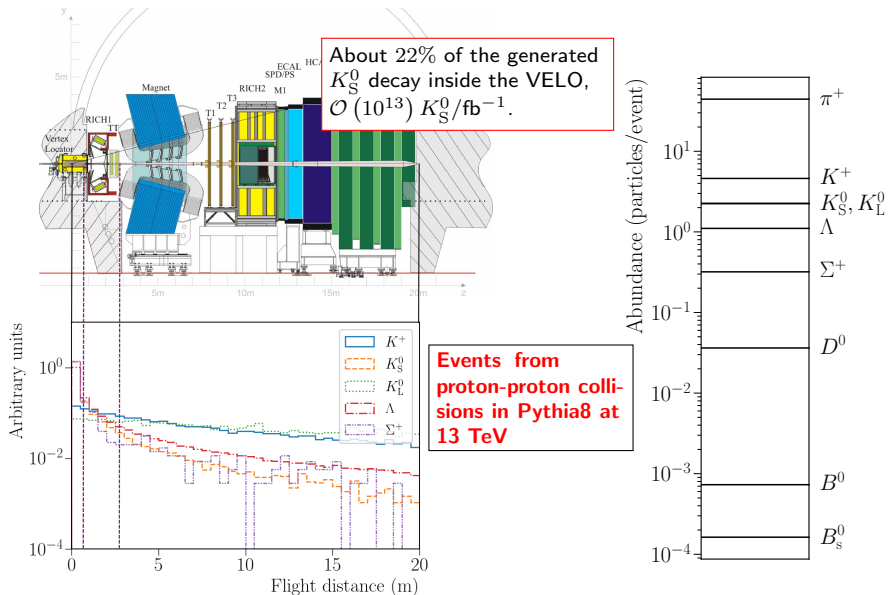
The LHCb detector



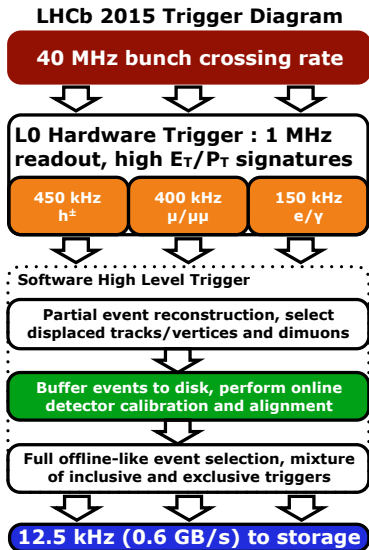
The LHCb detector



Production of strange hadrons at LHCb



The Run 2 trigger

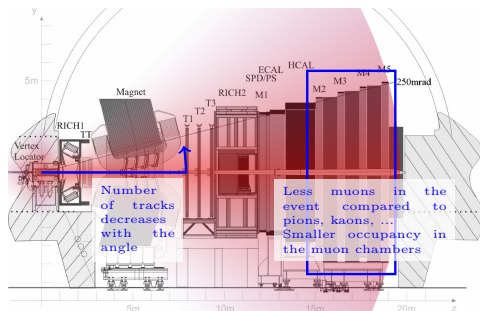


- The Run 1 trigger of 2011 was not optimized at all for strange decays.
- In 2012, the mass bounds for some selections were tuned at HLT1 and HLT2 to cover the K_S^0 mass.
- For Run 2, a special muon identification algorithm was introduced to select low- p_T muon at HLT1.
- The overall gain of efficiency was around one order of magnitude with respect to Run 1.
- Unfortunately, the L0 could not be changed/tuned, and is the main bottleneck for studies of strange decays.

Tracking for very low- p_T muons at the trigger level

Muon tracks from strange decays have lower transverse momentum (p_T), $\mathcal{O}(250)$ MeV/ c , than those from b and c hadron decays.

- Number of tracks (and combinations) to be processed per event drastically increases when p_T decreases.
- Profit from small occupancy in muon detectors to do a prompt muon identification.
- Implemented for 2016–2018 at HLT1.
- Constitutes one of the mayor differences with respect to Run-I (overall trigger efficiency increased by a factor ~ 8).

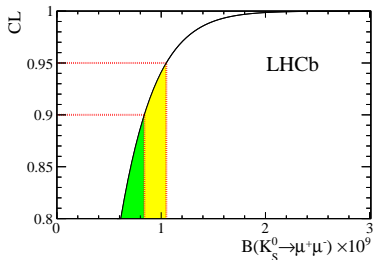


Include information from the muon chambers early in the reconstruction chain:

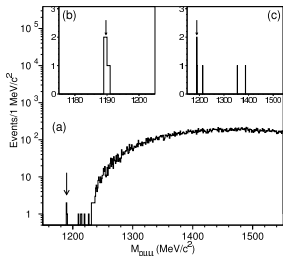


So far at LHCb...

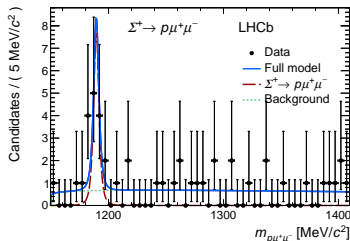
- The improved limits of the $K_S^0 \rightarrow \mu^+ \mu^-$ decay, complemented with the study of $\Sigma^+ \rightarrow p \mu^+ \mu^-$, showed the potentials of the LHCb detector to study strange decays.
- LHCb uncovered his physics range for **KAON 2016**.
- Several improvements took place for the start of Run 2 data-taking:
 - New trigger selections for dimuons, dielectrons and LFV modes (efficiencies $\times 10$).
 - Optimized VELO material description.
 - Muon-identification for low- p_T processes.



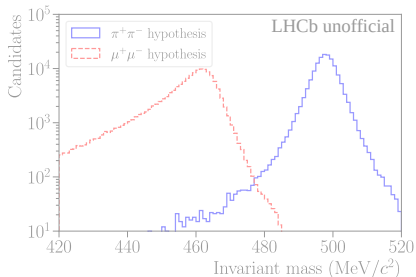
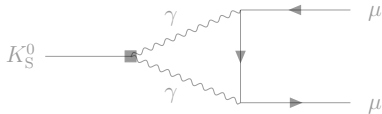
[JHEP 01 (2013) 090]



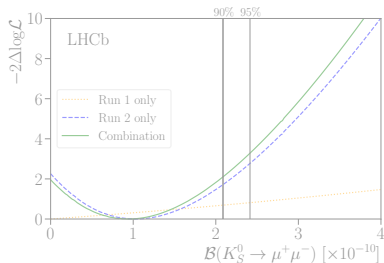
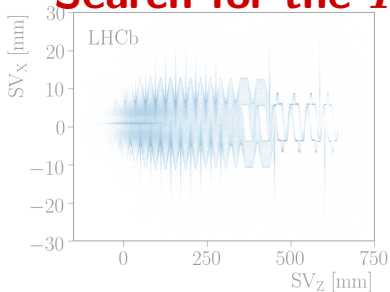
[Phys. Rev. Lett. 94]



[Phys. Rev. Lett. 120]



Search for the $K_S^0 \rightarrow \mu^+\mu^-$ decay



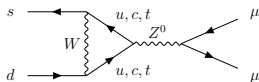
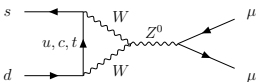
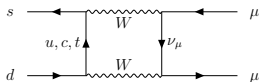
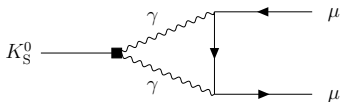
The $K_S^0 \rightarrow \mu^+ \mu^-$ decay

- The study of the $K_L^0 \rightarrow \mu^+ \mu^-$ decay lead to the introduction of the GIM mechanism and the prediction of the c quark.
- Flavor-changing neutral current decay, dominated by long-distance contributions.
- The K_S^0 mode is more suppressed than for the K_L^0 :

$$\mathcal{B}_{\text{exp.}} (K_L^0 \rightarrow \mu^+ \mu^-) = (6.84 \pm 0.11) \times 10^{-9} \quad \text{[PDG]}$$

$$\mathcal{B}_{\text{SM}} (K_S^0 \rightarrow \mu^+ \mu^-) = (5.18 \pm 1.50_{\text{LD}} \pm 0.02_{\text{SD}}) \times 10^{-12}$$

[JHEP05(2018)024], [JHEP0401(2004)009], [NPB366(1991)189]



The $K_S^0 \rightarrow \mu^+ \mu^-$ decay in the SM

The branching fraction of the K_S^0 (K_L^0) decay can be expressed as:

$$\mathcal{B}(K_{S/L}^0 \rightarrow \mu^+ \mu^-) \propto \frac{m_K \beta_\mu}{8\pi} (|A|^2 + \beta_\mu^2 |B|^2), \quad \beta_\mu = \sqrt{1 - \frac{4m_\mu^2}{m_K^2}}$$

where A and B describe the s -wave and p -wave components, respectively.

- A and B have opposite CP, being the first CP-conserving(violating) for the K_L^0 (K_S^0) and vice-versa.
- The process $K_{S/L} \rightarrow \gamma^* \gamma^*$ contributes to both amplitudes, but always with a negligible CP-violating contribution.
- Short-distance effects can only affect the A term.

The branching fraction evaluates to

$$\mathcal{B}(K_S^0 \rightarrow \mu^+ \mu^-) \propto \frac{m_K \beta_\mu}{8\pi} (|A_{\text{short}}|^2 + \beta_\mu^2 |B_{S,\gamma\gamma}|^2).$$

leading to

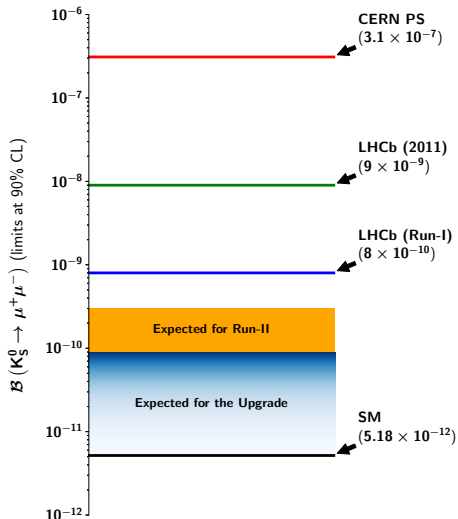
$$\mathcal{B}_{\text{SM}}(K_S^0 \rightarrow \mu^+ \mu^-) = (5.18 \pm 1.50_{\text{LD}} \pm 0.02_{\text{SD}}) \times 10^{-12}$$

The search for the $K_S^0 \rightarrow \mu^+ \mu^-$ decay

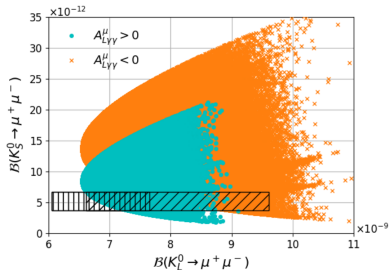
Need for a huge production of K_S^0 and a good muon identification in order to study this decay.

- First measurement from the 70s
[PLB 44 (1973) 217].
- No activity from the experimental side till the LHCb operation started.
- First measurement with data from 2011 [JHEP 01 (2013) 090].
- Full Run 1 result published in 2017 [EPJ-C (2017) 77:678].
- The study of the full Run 2 data sample is presented here [arXiv:2001.10354].

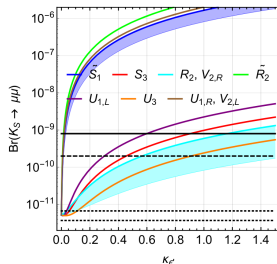
Still far from the SM prediction, but current bounds can help to discriminate among many BSM scenarios.



$K_S^0 \rightarrow \mu^+ \mu^-$ meets BSM physics



Implications in SUSY [JHEP05(2018)024].

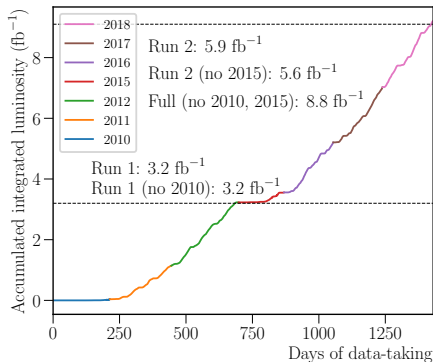
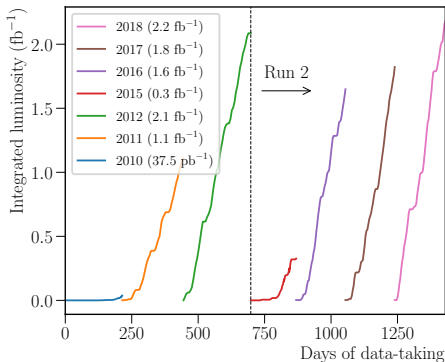


Implications in Leptoquark models [JHEP02(2018)101].

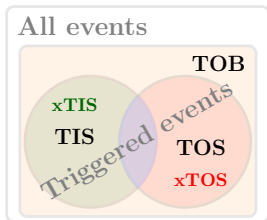
- $K_S^0 \rightarrow \mu^+ \mu^-$ is sensitive to different new-physics than $K_L^0 \rightarrow \mu^+ \mu^-$, in some models one order of magnitude greater.
- Implications in Supersymmetry and Leptoquark models, with connection to other observables like ϵ'/ϵ .

The search for $K_S^0 \rightarrow \mu^+ \mu^-$ with Run 2 data

- Analysis done using data from 2016–2018.
- Data from 2015 not included due to the reduced trigger efficiency and integrated luminosity.
- Including 2015 would improve the result by $\sim 0.05\%$ (negligible with respect to the rest of the data).
- Take into account the result from Run 1 using its posterior probability as a prior.



The trigger conditions in Run 2



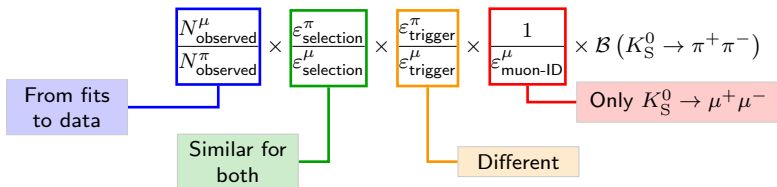
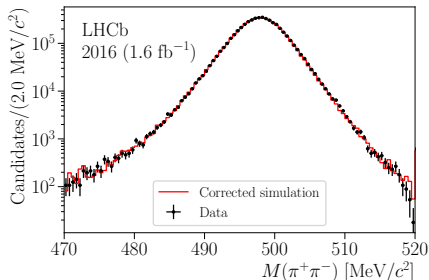
Categories defined by the $K_S^0 \rightarrow \mu^+ \mu^-$ candidate, depending whether it satisfies the trigger requirements or not:

- TIS: Triggered Independent of Signal.
- TOS: Triggered On Signal.
- TOB: Neither TIS nor TOS.

- L0 (hardware) could not be changed, but HLT1 and HLT2 were optimized.
- Analysis was done using two different trigger selections depending on the L0 requirements:
 - TIS: any candidate from an event surviving the L0 selections and satisfying the trigger requirements at the HLT.
 - xTOS: candidates from events surviving specific muonic trigger selections at all levels and not belonging to the TIS category.
- Candidates are required to satisfy the same HLT requirements for both categories (TOS at HLT).
- Events from the Minimum Bias (MB) stream were also used for normalization purposes.

The $K_S^0 \rightarrow \mu^+ \mu^-$ normalization

- Need to normalize to the K_S^0 production rate.
- LHC K_S^0 cross-section estimated to be ~ 0.6 barn.
- Low trigger efficiency for $K_S^0 \rightarrow \pi^+ \pi^-$ pushes to the use of candidates from the MB stream.
- Selection kept similar to $K_S^0 \rightarrow \mu^+ \mu^-$; most of the systematic uncertainties cancel in the ratio.



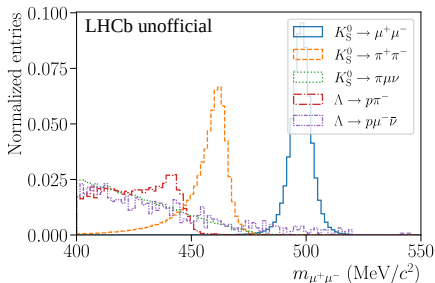
Backgrounds

- Due to the lower mass of the K_S^0 , less types of backgrounds are present with respect to b hadron decays:

$$B^0 \rightarrow K^{*0} \bar{K}^{*0} \Rightarrow B^0/B_s^0/\Lambda_b^0 \rightarrow hh'h''h'''$$

- However, due to the very low branching fraction $\sim 10^{-12}$, even suppressed backgrounds ($\mathcal{B} \sim 10^{-4}$) could overpass the selection requirements.
- Even processes like $B^0/D^0 \rightarrow \omega(782)(\rightarrow \pi^0 \mu^+ \mu^-)X$ could significantly contribute to the dimuon invariant mass signal region.

| Mode | Branching fraction |
|---|----------------------------------|
| $K_S^0 \rightarrow \pi^+ \pi^-$ | $(69.20 \pm 0.05)\%$ |
| $\Lambda \rightarrow p \pi^-$ | $(63.9 \pm 0.5)\%$ |
| $\Lambda \rightarrow p \mu^- \bar{\nu}$ | $(1.57 \pm 0.35) \times 10^{-4}$ |
| $K_S^0 \rightarrow \pi \mu \nu$ | $(4.56 \pm 0.20) \pm 10^{-4}$ |
| $K_L^0 \rightarrow \pi \mu \nu$ | $(27.04 \pm 0.07)\%$ |



Background from $\Lambda \rightarrow p\pi^-$ decays

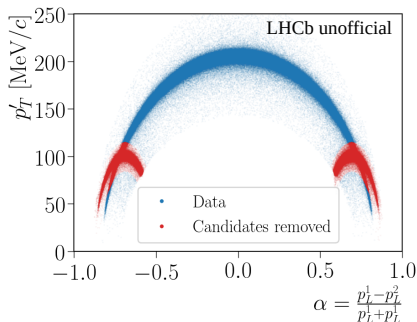
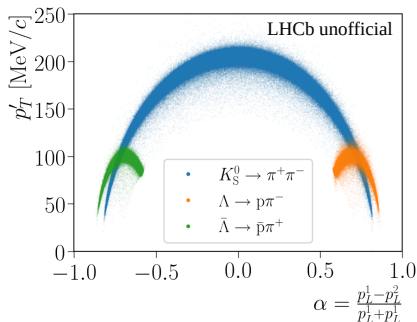
- $\Lambda \rightarrow p\pi^-$ is a dangerous background for $K_S^0 \rightarrow \pi^+\pi^-$ $\mathcal{B} = (63.9 \pm 0.5)\%$.
- For $K_S^0 \rightarrow \mu^+\mu^-$, the contribution from $\Lambda \rightarrow p\pi^-$ is removed by applying requirements in the dimuon invariant mass ($m_{\mu^+\mu^-} > 460 \text{ MeV}/c^2$).
- An additional selection based on the Armenteros-Podolanski method [Phil. Mag. 45 (1954) 13] is used to further reduce this background.

$$\left| \left[\left((\alpha \pm \alpha^*) \frac{M_\Lambda p_{K_S^0}}{2p^* \sqrt{p_{K_S^0}^2 + M_\Lambda^2}} \right)^2 + \left(\frac{p'_T}{p^*} \right)^2 \right] - 1 \right| > 0.3$$

where the momenta variables are taken with respect to the flight direction of the K_S^0 and

$$\alpha = \frac{p_L^1 - p_L^2}{p_L^1 + p_L^2} \quad \alpha^* \equiv \frac{M_p^2 - M_\pi^2}{M_\Lambda^2}$$
$$p^* \equiv \frac{(M_\Lambda^2 - M_p^2 - M_\pi^2)^2 - 4M_p^2 M_\pi^2}{4M_\Lambda^2}$$

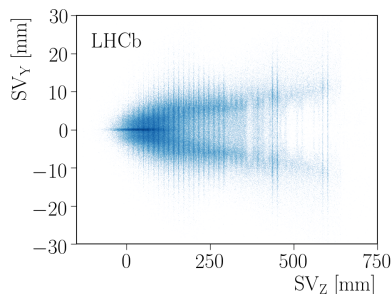
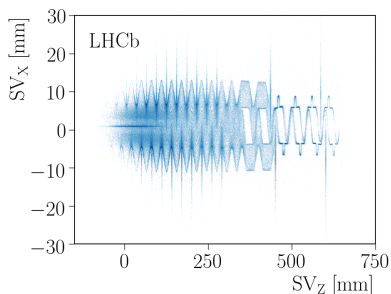
Background from $\Lambda \rightarrow p\pi^-$ decays



- This selection has an efficiency of $\sim 100\%$ for $K_S^0 \rightarrow \mu^+\mu^-$ and $K_S^0 \rightarrow \pi^+\pi^-$, reducing the $\Lambda \rightarrow p\pi^-$ contribution to negligible levels.
- The $\Lambda \rightarrow p\mu\nu$ decay is more suppressed $\mathcal{B} = (1.57 \pm 0.35) \times 10^{-4}$, and its contribution is similarly reduced.

Inelastic interactions with the detector material

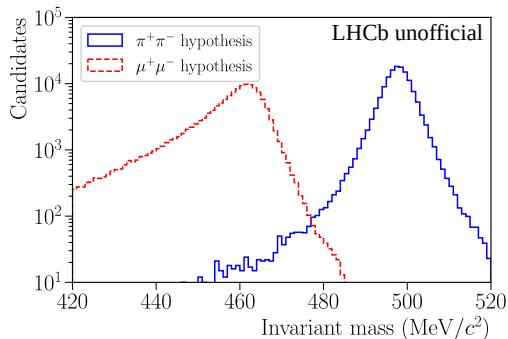
The pattern of the VELO can be clearly seen when looking at the vertices of candidates with $m_{\mu^+\mu^-} > 520 \text{ MeV}/c^2$:



- These vertices arise from inelastic interactions with the VELO material.
- New description of the VELO material and RF foil [[JINST 13 P06008](#)].
- Possibility to calculate the probability of a candidate to belong to a material interaction.
- Exploit its power on a MVA analysis to fight also against background from combinatorics.

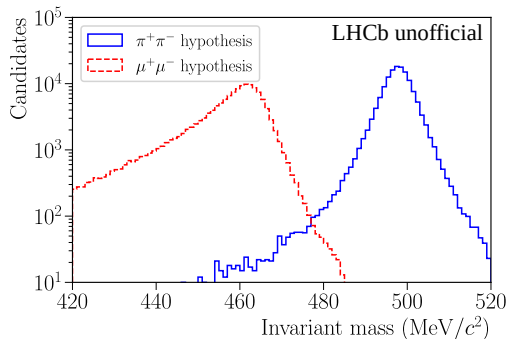
The doubly misidentified $K_S^0 \rightarrow \pi^+\pi^-$ background

- Main background comes from misidentification of pions as muons.
- $K_S^0 \rightarrow \pi^+\pi^-$ dominates and is the most abundant background.
- Mass shifted to the left by $\sim 40 \text{ MeV}/c^2$ ($10 \times$ the resolution!).
- Residual contribution from $K^0 \rightarrow \pi\mu\nu$, indistinguishable from $K_S^0 \rightarrow \pi^+\pi^-$.

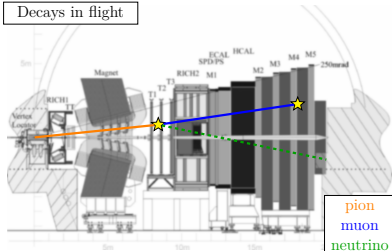


The doubly misidentified $K_S^0 \rightarrow \pi^+\pi^-$ background

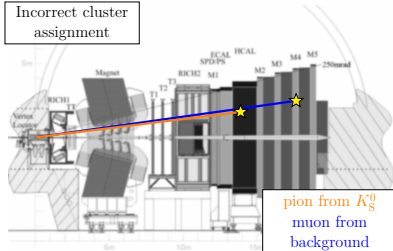
- Main background comes from misidentification of pions as muons.
- $K_S^0 \rightarrow \pi^+\pi^-$ dominates and is the most abundant background.
- Mass shifted to the left by $\sim 40 \text{ MeV}/c^2$ ($10 \times$ the resolution!).
- Residual contribution from $K^0 \rightarrow \pi\mu\nu$, indistinguishable from $K_S^0 \rightarrow \pi^+\pi^-$.



Decays in flight



Incorrect cluster assignment



Backgrounds from other strange decays

- Irreducible background.
- $\mathcal{B}_{\text{eff.}}(K_L^0 \rightarrow \mu^+\mu^-) \sim 10^{-11}$.
- 5 SM candidates expected in the final data set.
- Considered in the dimuon mass fit.

| Decay | Branching fraction |
|------------------------------------|------------------------------------|
| $K_L^0 \rightarrow \mu^+\mu^-$ | $(6.84 \pm 0.11) \times 10^{-9}$ |
| $K^0 \rightarrow \mu^+\mu^-\gamma$ | ———— |
| $K^+ \rightarrow \pi^+\mu^+\mu^-$ | $(9.4 \pm 0.6) \times 10^{-8}$ |
| $\Sigma^+ \rightarrow p\mu^+\mu^-$ | $2.2^{+1.8}_{-1.3} \times 10^{-8}$ |

Values from [PDG](#)

Backgrounds from other strange decays

- Irreducible background.
- $\mathcal{B}_{\text{eff.}}(K_L^0 \rightarrow \mu^+ \mu^-) \sim 10^{-11}$.
- 5 SM candidates expected in the final data set.
- Considered in the dimuon mass fit.

- $\mathcal{B}_{\text{SM}}(K_S^0 \rightarrow \mu^+ \mu^- \gamma) = (1.45 \pm 0.27) \times 10^{-9}$
- $\mathcal{B}(K_L^0 \rightarrow \mu^+ \mu^- \gamma) = (3.59 \pm 0.11) \times 10^{-7}$
- Dimuon spectrum displaced to the left, no candidates in the fit region.
- $K_S^0 \rightarrow \mu^+ \mu^- \gamma \gamma$ even more suppressed.

| Decay | Branching fraction |
|--------------------------------------|------------------------------------|
| $K_L^0 \rightarrow \mu^+ \mu^-$ | $(6.84 \pm 0.11) \times 10^{-9}$ |
| $K^0 \rightarrow \mu^+ \mu^- \gamma$ | — |
| $K^+ \rightarrow \pi^+ \mu^+ \mu^-$ | $(9.4 \pm 0.6) \times 10^{-8}$ |
| $\Sigma^+ \rightarrow p \mu^+ \mu^-$ | $2.2^{+1.8}_{-1.3} \times 10^{-8}$ |

Values from [PDG](#)

Backgrounds from other strange decays

- Irreducible background.
- $\mathcal{B}_{\text{eff.}}(K_L^0 \rightarrow \mu^+\mu^-) \sim 10^{-11}$.
- 5 SM candidates expected in the final data set.
- Considered in the dimuon mass fit.

- Very rare decays.
- Dimuon mass below the thresholds.

- $\mathcal{B}_{\text{SM}}(K_S^0 \rightarrow \mu^+\mu^-\gamma) = (1.45 \pm 0.27) \times 10^{-9}$
- $\mathcal{B}(K_L^0 \rightarrow \mu^+\mu^-\gamma) = (3.59 \pm 0.11) \times 10^{-7}$
- Dimuon spectrum displaced to the left, no candidates in the fit region.
- $K_S^0 \rightarrow \mu^+\mu^-\gamma\gamma$ even more suppressed.

| Decay | Branching fraction |
|------------------------------------|------------------------------------|
| $K_L^0 \rightarrow \mu^+\mu^-$ | $(6.84 \pm 0.11) \times 10^{-9}$ |
| $K^0 \rightarrow \mu^+\mu^-\gamma$ | — |
| $K^+ \rightarrow \pi^+\mu^+\mu^-$ | $(9.4 \pm 0.6) \times 10^{-8}$ |
| $\Sigma^+ \rightarrow p\mu^+\mu^-$ | $2.2^{+1.8}_{-1.3} \times 10^{-8}$ |

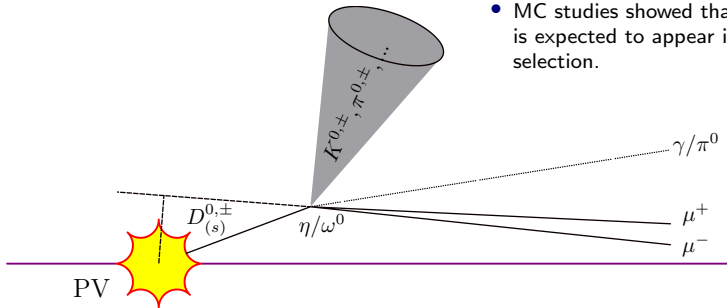
Values from [PDG](#)

Backgrounds from resonances

Decays from resonances have been considered as possible backgrounds [PDG]:

| Decay | Branching fraction |
|---|----------------------------------|
| $\omega(782) \rightarrow \pi^0 \mu^+ \mu^-$ | $(1.34 \pm 0.18) \times 10^{-4}$ |
| $\eta \rightarrow \mu^+ \mu^- \gamma$ | $(3.1 \pm 0.4) \times 10^{-4}$ |
| $\omega(782) \rightarrow \pi^0 \pi^+ \pi^-$ | $(89.3 \pm 0.6) \%$ |
| $\eta \rightarrow \pi^+ \pi^- \gamma$ | $(4.22 \pm 0.08) \%$ |

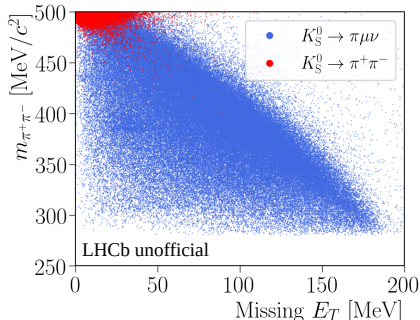
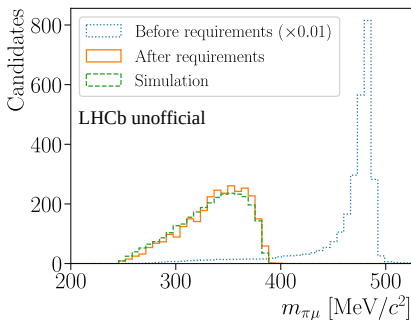
- These resonances decay promptly.
- Only those coming from c and b hadron decays could survive the trigger and selection requirements.
- Decays in the pionic mode are not visible in the $K_S^0 \rightarrow \pi^+ \pi^-$ selection.
- MC studies showed that none of them is expected to appear in the final selection.



Cross-checks on data

- Some systematic uncertainties were evaluated using $K_S^0 \rightarrow \pi^+\pi^-$, $K^0 \rightarrow \pi\mu\nu$ and $J/\psi \rightarrow \mu^+\mu^-$ data/MC candidates.
- Different kinematics and p_T spectrum for $K^0 \rightarrow \pi\mu\nu$ and $J/\psi \rightarrow \mu^+\mu^-$.
- The $K_S^0 \rightarrow \pi\mu\nu$ decay has been recently discovered by KLOE2 [[arXiv:1912.05990](https://arxiv.org/abs/1912.05990)]; at LHCb, such candidates can be seen already in trigger-unbiased events.

$$\mathcal{B}(K_S^0 \rightarrow \pi\mu\nu) = (4.56 \pm 0.11 \pm 0.17) \times 10^{-4}$$



Systematic uncertainties

Biggest systematic uncertainty comes from the determination of the trigger efficiency:

- Hardware trigger (L0): 11%
- Software trigger (HLT): 13%

Other sources of systematic uncertainties are:

- Efficiency of the muon-identification 4 – 12%, cross-checked using $J/\psi \rightarrow \mu^+\mu^-$ real and simulated data. Low statistics for low- p_T muons, so also need to use $K_S^0 \rightarrow \pi\mu\nu$ to cross-check.
- Systematic uncertainty on the correction for data-simulation differences, 6%.
- BDT response across the years, 5%.
- Efficiency ratio between $K_S^0 \rightarrow \mu^+\mu^-$ and $K_S^0 \rightarrow \pi^+\pi^-$ with and without weights, 3%.
- Determination of the no-bias trigger rates $< 1\%$.

Total systematic varies between 19% and 23%, depending on the trigger category and BDT bin. Lowest values are in the TIS category and higher BDT bins.

The dimuon invariant mass fit model

Signal

- Hypatia distribution [arXiv:1312.5000].
- Checks for data/MC agreement for the signal mass shape on $K_S^0 \rightarrow \pi^+\pi^-$.
- Extrapolate results from $K_S^0 \rightarrow \pi^+\pi^-$ to $K_S^0 \rightarrow \mu^+\mu^-$.

$K_L^0 \rightarrow \mu^+\mu^-$

- Same shape as the signal (indistinguishable).
- Constrained given $\mathcal{B}(K_L^0 \rightarrow \mu^+\mu^-) = (6.84 \pm 0.11)^{-9}$

Fit model

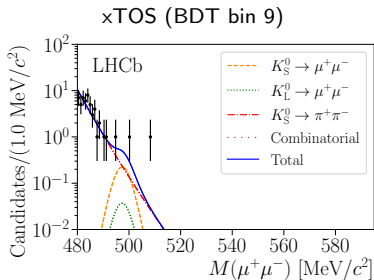
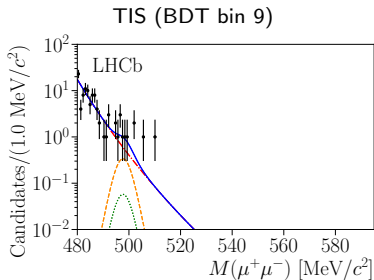
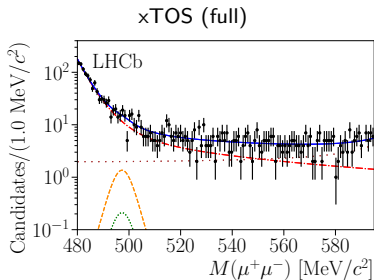
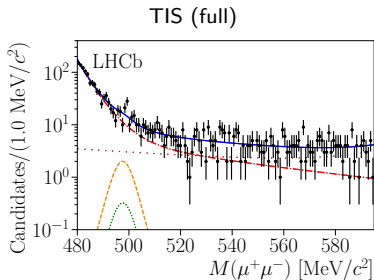
$K_S^0 \rightarrow \pi^+\pi^- / K^0 \rightarrow \pi\mu\nu$

- Parameterized using a power-law $f(x) = (x - m)^{-n}$.
- Shape of no-, single- and double-misidentification studied in fast simulation and validated in data.
- $K_S^0 \rightarrow \pi\mu\nu$ absorbed by it.

Combinatorics and material interactions

- Exponential distribution.
- Validated using right-sideband candidates.

Fit to the dimuon invariant mass spectrum



Signal yield and limit calculation

- The total number of observed $K_S^0 \rightarrow \mu^+ \mu^-$ candidates is 34 ± 23 .
- The limit is calculated from the $\log \mathcal{L}$ profile of the branching fraction.

- Integrating the profile yields

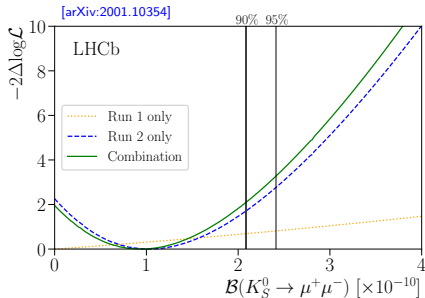
$$\mathcal{B}(K_S^0 \rightarrow \mu^+ \mu^-) < 2.2 \times 10^{-10} \text{ at 90\% CL}$$

- Combined with the Run 1 result (including its posterior probability as a prior)

$$\mathcal{B}(K_S^0 \rightarrow \mu^+ \mu^-) < 2.1 \times 10^{-10} \text{ at 90\% CL}$$

- In addition, a result on the $K_L^0 \rightarrow \mu^+ \mu^-$ mode is also computed rerunning the fit with a single signal component:

$$\mathcal{B}(K_L^0 \rightarrow \mu^+ \mu^-) = 5.0_{-2.9}^{+3.2} \times 10^{-8}$$



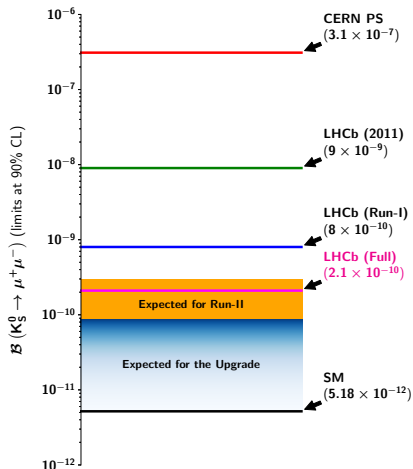
$$\frac{\int_0^\beta \mathcal{L}(\mathcal{B}) d\mathcal{B}}{\int_0^\infty \mathcal{L}(\mathcal{B}) d\mathcal{B}} = 1 - \alpha = 90\%$$

$$\frac{\int_0^\beta p(\mathcal{B}) \mathcal{L}(\mathcal{B}) d\mathcal{B}}{\int_0^\infty p(\mathcal{B}) \mathcal{L}(\mathcal{B}) d\mathcal{B}} = 1 - \alpha = 90\%$$

Run 1 posterior

The future of $K_S^0 \rightarrow \mu^+ \mu^-$

- No significant signal observed so far.
- Limit brought down to
$$\mathcal{B}(K_S^0 \rightarrow \mu^+ \mu^-) = 2.1 \times 10^{-10} \text{ at 90\% CL}$$
- The design of the Upgrade trigger is crucial for this kind of searches.
- In the best scenario (same performance as in Run 2), we would be entering into a very interesting region $\mathcal{B}(K_S^0 \rightarrow \mu^+ \mu^-) \sim 10^{-11}$.
- However, the standard model value might only be reachable on the LHCb Phase-II Upgrade.



PEOPLE ARE STRANGE

B/W UNHAPPY GIRL

EK-45621

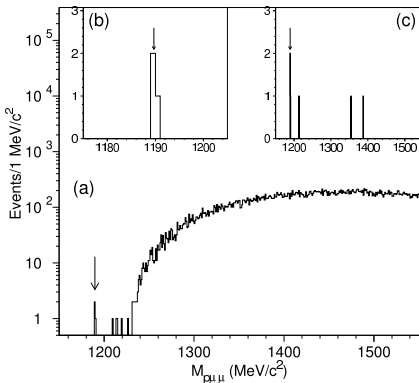
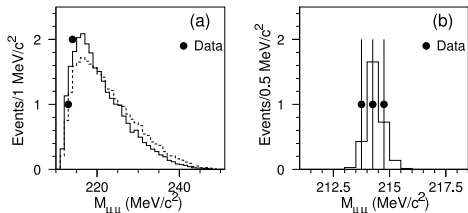
THE
doors

Other strange decays at LHCb



$\Sigma^+ \rightarrow p\mu^+\mu^-$

- Evidence for this decay was found by the HyperCP experiment with **3 events in absence of background**
- Branching fraction in agreement with SM
 $\mathcal{B}(\Sigma^+ \rightarrow p\mu^+\mu^-) = (8.6_{-5.4}^{+6.6} \pm 5.5) \times 10^{-8}$
- The three events had the **same dimuon invariant mass**, thus pointing towards a $\Sigma^+ \rightarrow pX^0(\rightarrow \mu^+\mu^-)$ decay.

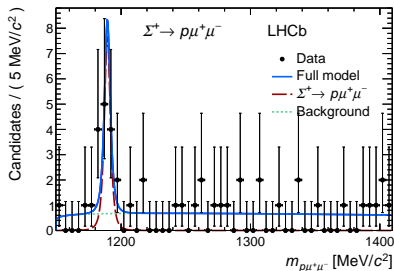


[Phys. Rev. Lett. 94]

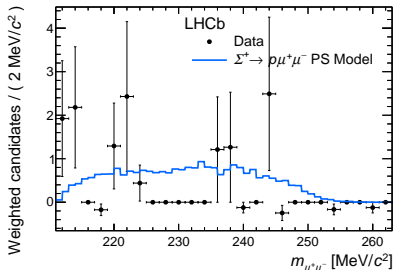
$$\mathcal{B}(\Sigma^+ \rightarrow pX^0(\rightarrow \mu^+\mu^-)) = (3.1_{-1.9}^{+2.4} \pm 5.5) \times 10^{-8}$$

$\Sigma^+ \rightarrow p\mu^+\mu^-$

- Using full Run 1 statistics (3 fb^{-1}).
- Two analysis strategies adopted: branching fraction measurement, dimuon-mass analysis.
- Normalization to $\Sigma^+ \rightarrow p\pi^0$.
- Cross-checks and systematics calculated using also $K^+ \rightarrow \pi^+\pi^-\pi^+$.



[Phys. Rev. Lett. 120]



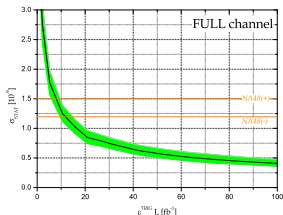
- Evidence of the $\Sigma^+ \rightarrow p\mu^+\mu^-$ decay at 4.1σ .

$$\mathcal{B}(\Sigma^+ \rightarrow p\mu^+\mu^-) = 2.2^{+1.8}_{-1.3} \times 10^{-8}$$

- The Hyper-CP anomaly is not confirmed:

$$\mathcal{B}(\Sigma^+ \rightarrow pX^0(\rightarrow \mu^+\mu^-)) < 1.4 \times 10^{-8} \text{ at } 90\%$$

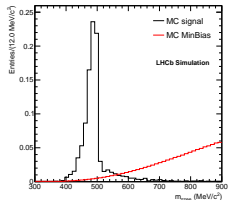
Possible studies at LHCb in Run 1/2



[CERN-LHCb-PUB-2016-017]

- Increase the precision of $K_S^0 \rightarrow \pi^0 \mu^+ \mu^-$ (needed for the SM prediction of $K_L^0 \rightarrow \pi^0 \mu^+ \mu^-$).
- Can omit the π^0 reconstruction.
- Explore also $K_S^0 \rightarrow \mu^+ \mu^- \gamma$.

- $K_S^0 \rightarrow \pi^+ \pi^- e^+ e^-$ needed to normalize $K_S^0 \rightarrow \ell \ell' \ell' e'$ modes ($\mathcal{B} \sim 10^{-13}$).
- \mathcal{B} measured by NA48 [PLB vol. 694 pages 301-309].
- Seen this decay is possible with Run 1/2 data.



[LHCb-PUB-2016-016]

| | $\Lambda \rightarrow p$ | $\Sigma^- \rightarrow n$ | $\Xi^0 \rightarrow \Sigma^+$ | $\Xi^- \rightarrow \Lambda$ |
|--------|-------------------------|--------------------------|------------------------------|-----------------------------|
| Expt. | 0.189(41) | 0.442(39) | 0.0092(14) | 0.6(5) |
| SM-NLO | 0.153(8) | 0.444(22) | 0.0084(4) | 0.275(14) |

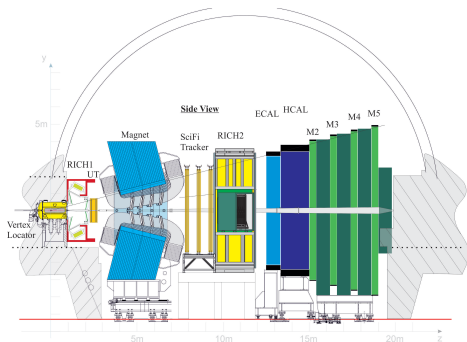
- Semileptonic hyperon decays (SHD) allow to explore tensor parts in NP models.
- Measurements in the muonic modes are old and have low precision ($\sigma \sim 10\%$).
- Alternative measurement of $|V_{us}|$.



**Trigger developments
for the LHCb upgrade**

The upgrade of the LHCb experiment

| 2019 | 2020 | 2021 | 2022 | 2023 | 2024 | 2025 | 2026 | 2027 | 2028 | 2029 | 2030 | 2031 | 2032 | ... |
|------------------------------|------|---|------|------|------------------------------|------|------|--|------|------|-----------------------|------|--|-----|
| LS2 | | Run 3 | | | LS3 | | | Run 4 | | | LS4 | | Run 5 | |
| LHCb 40 Mhz Upgrade Phase 1a | | $L = 2 \times 10^{33}$ | | | LHCb 40 MHz Upgrade Phase 1b | | | $L = 2 \times 10^{33}$ 50 fb^{-1} | | | LHCb Upgrade Phase II | | $L = 2 \times 10^{34}$ 300 fb^{-1} | |
| ATLAS Upgrade Phase I | | $L = 2 \times 10^{34}$ 300 fb^{-1} | | | ATLAS Upgrade Phase II | | | HL-LHC $L = 5 \times 10^{34}$ | | | ATLAS | | HL-LHC $L = 5 \times 10^{34}$ 3000 fb^{-1} | |
| CMS Upgrade Phase I | | | | | CMS Upgrade Phase II | | | | | | CMS | | | |
| Belle II | | 5 ab^{-1} $L = 8 \times 10^{35}$ | | | 50 ab^{-1} | | | | | | | | | |



- Luminosity increases by a factor 5:
 $4 \times 10^{32} \text{ cm}^{-2}\text{s}^{-1} \rightarrow 2 \times 10^{33} \text{ cm}^{-2}\text{s}^{-1}$.
- Major modifications in the tracking subdetectors.
- All the readout and electronics is changed.
- Taking data at 30 MHz, a challenge from the computational point of view.

The trigger in the upgrade

Run-II conditions 2015-2018

LHCb 2015 Trigger Diagram

40 MHz bunch crossing rate

L0 Hardware Trigger : 1 MHz readout, high E_T/P_T signatures

450 kHz
 h^\pm

400 kHz
 $\mu/\mu\mu$

150 kHz
 e/γ

Software High Level Trigger

Partial event reconstruction, select displaced tracks/vertices and dimuons

Buffer events to disk, perform online detector calibration and alignment

Full offline-like event selection, mixture of inclusive and exclusive triggers

12.5 kHz (0.6 GB/s) to storage

Upgrade conditions (ongoing)

LHCb Upgrade Trigger Diagram

30 MHz inelastic event rate
(full rate event building)

Software High Level Trigger

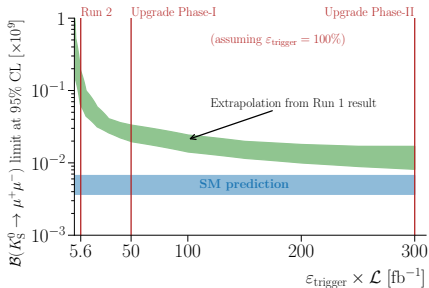
Full event reconstruction, inclusive and exclusive kinematic/geometric selections

Buffer events to disk, perform online detector calibration and alignment

Add offline precision particle identification and track quality information to selections
Output full event information for inclusive triggers, trigger candidates and related primary vertices for exclusive triggers

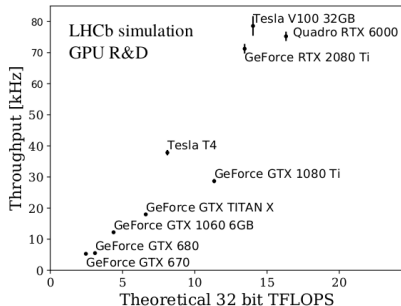
2-5 GB/s to storage

Prospects for strange decays in the upgrade



- The implementation of the upgrade HLT1 on GPUs has been officially approved [[arXiv:1912.09161](https://arxiv.org/abs/1912.09161)].
- Unprecedented in particle physics, and might be one of the biggest GPU clusters in the world.
- Possibility to remove any kind of thresholds (efficiencies can easily grow by one order of magnitude with respect to the CPU).

- Having a full software trigger increases the flexibility of the detector to study strange decays.
- However, the VELO-UT tracking at low p_T should be revisited in order to improve the performance.
- In particular, for $K_S^0 \rightarrow \mu^+ \mu^-$, the region $\mathcal{B} \sim 10^{-11}$ can be accessed.



The LHCb experiment can widely complement the search for strange decays of other (smaller) experiments:

- Can drastically improve the results for K_S^0 mesons.
- The study of hyperon decays in the future might be territory of LHCb only.
- Low background levels in most decays.

| Channel | \mathcal{R} | ϵ_L | ϵ_D | σ_L (MeV/c ²) | σ_D (MeV/c ²) |
|--|---------------|-----------------------------|---------------------------|----------------------------------|----------------------------------|
| $K_S^0 \rightarrow \mu^+ \mu^-$ | 1 | 1.0 (1.0) | 1.8 (1.8) | ~ 3.0 | ~ 8.0 |
| $K_S^0 \rightarrow \pi^+ \pi^-$ | 1 | 1.1 (0.30) | 1.9 (0.91) | ~ 2.5 | ~ 7.0 |
| $K_S^0 \rightarrow \pi^0 \mu^+ \mu^-$ | 1 | 0.93 (0.93) | 1.5 (1.5) | ~ 35 | ~ 45 |
| $K_S^0 \rightarrow \gamma \mu^+ \mu^-$ | 1 | 0.85 (0.85) | 1.4 (1.4) | ~ 60 | ~ 60 |
| $K_S^0 \rightarrow \mu^+ \mu^- \mu^+ \mu^-$ | 1 | 0.37 (0.37) | 1.1 (1.1) | ~ 1.0 | ~ 6.0 |
| $K_L^0 \rightarrow \mu^+ \mu^-$ | ~ 1 | $2.7 (2.7) \times 10^{-3}$ | 0.014 (0.014) | ~ 3.0 | ~ 7.0 |
| $K^+ \rightarrow \pi^+ \pi^+ \pi^-$ | ~ 2 | $9.0 (0.75) \times 10^{-3}$ | $41 (8.6) \times 10^{-3}$ | ~ 1.0 | ~ 4.0 |
| $K^+ \rightarrow \pi^+ \mu^+ \mu^-$ | ~ 2 | $6.3 (2.3) \times 10^{-3}$ | 0.030 (0.014) | ~ 1.5 | ~ 4.5 |
| $\Sigma^+ \rightarrow p \mu^+ \mu^-$ | ~ 0.13 | 0.28 (0.28) | 0.64 (0.64) | ~ 1.0 | ~ 3.0 |
| $\Lambda \rightarrow p \pi^-$ | ~ 0.45 | 0.41 (0.075) | 1.3 (0.39) | ~ 1.5 | ~ 5.0 |
| $\Lambda \rightarrow p \mu^- \bar{\nu}_\mu$ | ~ 0.45 | 0.32 (0.31) | 0.88 (0.86) | – | – |
| $\Xi^- \rightarrow \Lambda \mu^- \bar{\nu}_\mu$ | ~ 0.04 | $39 (5.7) \times 10^{-3}$ | 0.27 (0.09) | – | – |
| $\Xi^- \rightarrow \Sigma^0 \mu^- \bar{\nu}_\mu$ | ~ 0.03 | $24 (4.9) \times 10^{-3}$ | 0.21 (0.068) | – | – |
| $\Xi^- \rightarrow p \pi^- \pi^-$ | ~ 0.03 | 0.41(0.05) | 0.94 (0.20) | ~ 3.0 | ~ 9.0 |
| $\Xi^0 \rightarrow p \pi^-$ | ~ 0.03 | 1.0 (0.48) | 2.0 (1.3) | ~ 5.0 | ~ 10 |
| $\Omega^- \rightarrow \Lambda \pi^-$ | ~ 0.001 | $95 (6.7) \times 10^{-3}$ | 0.32 (0.10) | ~ 7.0 | ~ 20 |

| Channel | \mathcal{R} | ϵ_L | ϵ_D | $\sigma_L(\text{MeV}/c^2)$ | $\sigma_D(\text{MeV}/c^2)$ |
|--------------------------------------|---------------|------------------------|----------------------------------|----------------------------|----------------------------|
| $K_S^0 \rightarrow \pi^+\pi^-e^+e^-$ | 1 | 1.0 (0.18) | 2.83 (1.1) | ~ 2.0 | ~ 10 |
| $K_S^0 \rightarrow \mu^+\mu^-e^+e^-$ | 1 | 1.18 (0.48) | 2.93 (1.4) | ~ 2.0 | ~ 11 |
| $K^+ \rightarrow \pi^+e^+e^-$ | ~ 2 | 0.04 (0.01) | 0.17 (0.06) | ~ 3.0 | ~ 13 |
| $\Sigma^+ \rightarrow pe^+e^-$ | ~ 0.13 | 1.76 (0.56) | 3.2 (1.3) | ~ 3.5 | ~ 11 |
| $\Lambda \rightarrow p\pi^-e^+e^-$ | ~ 0.45 | $< 2.2 \times 10^{-4}$ | $\sim 17 (< 2.2) \times 10^{-4}$ | – | – |

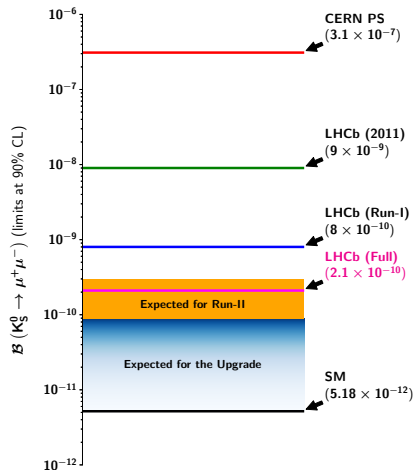
| Channel | \mathcal{R} | ϵ_L | ϵ_D | $\sigma_L(\text{MeV}/c^2)$ | $\sigma_D(\text{MeV}/c^2)$ |
|---------------------------------|---------------|----------------------------|---------------------------|----------------------------|----------------------------|
| $K_S^0 \rightarrow \mu^+e^-$ | 1 | 1.0 (0.84) | 1.5 (1.3) | ~ 3.0 | ~ 8.0 |
| $K_L^0 \rightarrow \mu^+e^-$ | 1 | $3.1 (2.6) \times 10^{-3}$ | $13 (11) \times 10^{-3}$ | ~ 3.0 | ~ 7.0 |
| $K^+ \rightarrow \pi^+\mu^+e^-$ | ~ 2 | $3.1 (1.1) \times 10^{-3}$ | $16 (8.5) \times 10^{-3}$ | ~ 2.0 | ~ 8.0 |

Summary

- Profiting from the large production of strange hadrons at LHCb, we can consider it as a strange-factory.
- The efficiency to study strange decays at LHCb is highly influenced by the design of its trigger.
- We are making giant steps towards the SM prediction of $K_S^0 \rightarrow \mu^+ \mu^-$!

$$\mathcal{B}(K_S^0 \rightarrow \mu^+ \mu^-) < 2.1 \times 10^{-10} \text{ at 90\% CL}$$

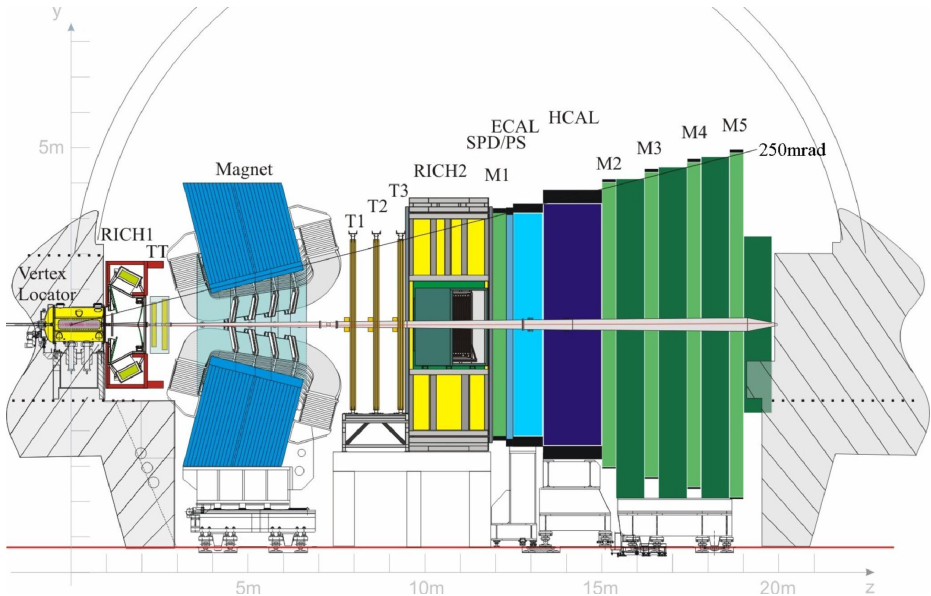
- Currently allowing to reduce the available variable-space for SUSY and leptoquark models.
- A promising environment to study more strange decays is foreseen at LHCb.
- Important contributions can be done at LHCb in mid- and long-terms.



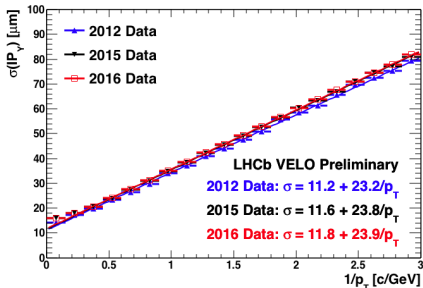
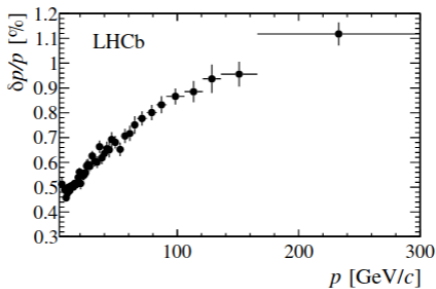
Thanks for your attention!

BACKUP

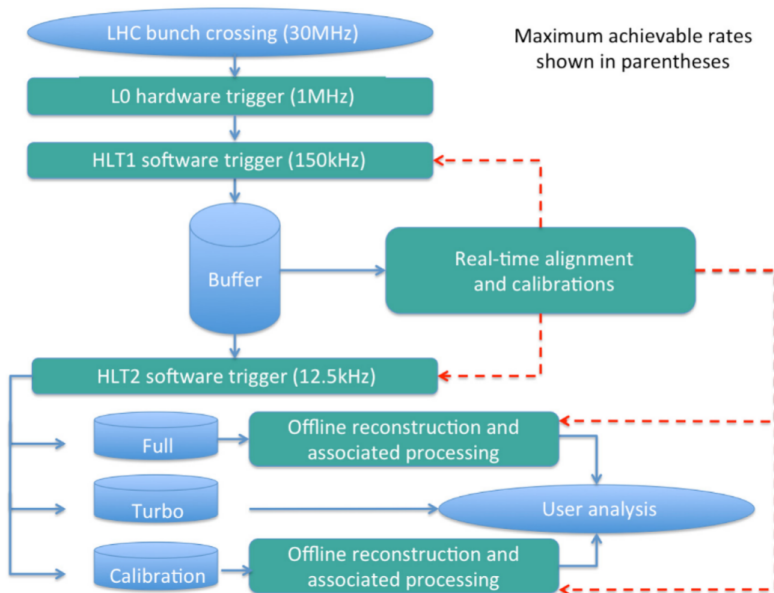
The LHCb detector



Momentum and impact parameter resolutions



The data flow in Run 2



Run 1 result of $K_S^0 \rightarrow \mu^+ \mu^-$

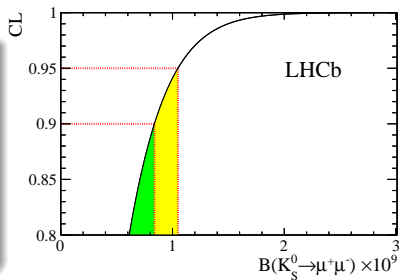
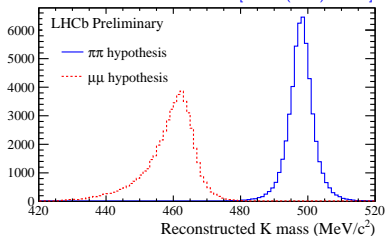
- Combination of the result from 2012 with that of 2011.
- HLT more efficient with respect to 2011, but not optimized for strange decays.
- The limit was improved by one order of magnitude with respect to 2011-only

$$\mathcal{B}(K_S^0 \rightarrow \mu^+ \mu^-) = 8 \times 10^{-10} \text{ at } 90\% \text{CL}$$

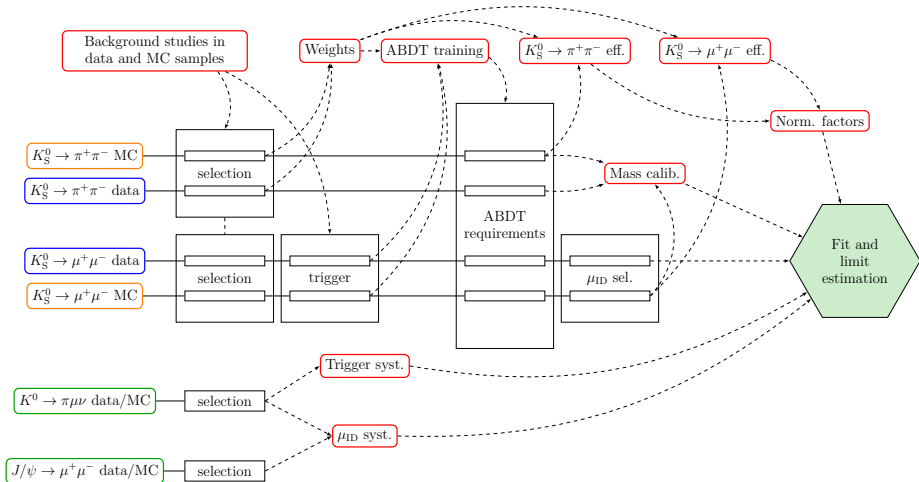
Contribution

- One of the main contributors.
- Worked in data processing, offline selection, fit model and limit calculation.
- Published in [EPJ-C](#).
- Highlighted at the [KAON conference of 2016](#).

[EPJ-C (2017) 77:678]



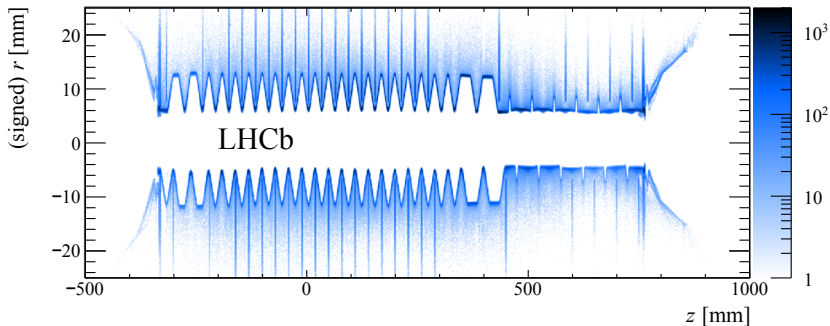
The analysis strategy



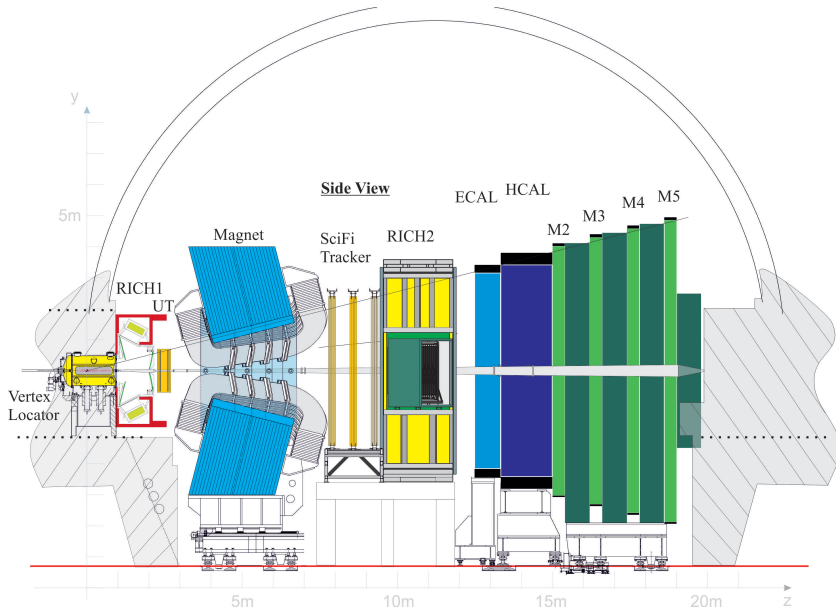
Inelastic interactions with the detector material

- New description of the VELO material and RF foil [JINST 13 P06008] allows to discriminate better our signal against this type of background.
- Probability of a candidate to come from a material interaction given by the uncertainty-weighted distance to the material:

$$D = \sqrt{\left(\frac{x - SV_x}{\sigma_x}\right)^2 + \left(\frac{y - SV_y}{\sigma_y}\right)^2 + \left(\frac{z - SV_z}{\sigma_z}\right)^2}$$



The upgraded LHCb detector



The data flow in Run 3

